



## CHARACTERISATION OF CHITOSAN EXTRACTED ENZYMATICALLY FROM SHRIMP SHELL WASTE, AND STUDY OF ITS ANTIOXIDANT POWER

Fatma KHAOUANI<sup>1</sup> and Atiqa KHERBECHE<sup>2</sup>

<sup>1,2</sup> Functional agrosystems and agronomic supply chain technologies Laboratory (AFTAGRO), University Abou Bakr Belkaid, Tlemcen, 13000, Algeria

\*Corresponding author: Dr Fatma KHAOUANI : [fatima.khaouani@univ-tlemcen.dz](mailto:fatima.khaouani@univ-tlemcen.dz)

### Article History

Volume 6, Issue 10, 2024

Received: 17 Apr 2024

Accepted : 03 May 2024

Doi :10.33472/AFJBS.6.10.2024.510-519

### ABSTRACT

The research aimed to identify shrimp shell detritus and extract chitosan using an enzyme. We analyzed the molecular weight, liquid volume, protein concentration, and ash content of chitosan. Chitosan production was at  $17.16 \pm 0.21\%$ , with an expected water content of  $7.32 \pm 0.05\%$ . The demineralization process resulted in an ash concentration ( $0.1114 \pm 0.002\%$ ) significantly lower than the 1% limit. Deproteinization revealed a protein concentration of  $1.12 \pm 0.02\%$ , with approximately  $97.02 \pm 0.05\%$  of the chemical being soluble. The average molecular mass was  $109.27 \pm 0.34$  KDa. Fourier transform infrared spectroscopy (FTIR) and XRD diffraction pattern analysis helped understand the chemical makeup, functional groups, and crystal structure of chitosan. Its antioxidant capabilities were tested using the DPPH technique, showing a 72% scavenging capacity and potent antioxidant activity similar to BHA at a concentration of 1%. These studies demonstrate the multiple potential uses of chitosan.

Keywords: Shrimp Shells, enzymatic extraction, chitosan, characterisation, antioxidant activity

## 1. INTRODUCTION

Chitosan is a natural polymer of marine origin, primarily extracted from the shells of crustaceans such as shrimp and crabs (Hahn, 1994; Kurita, 2006). This polysaccharide, composed of glucosamine and N-acetylglucosamine residues, is renowned for its biocompatibility, biodegradability, and antimicrobial properties, making it particularly interesting for various sectors such as agriculture, food, medicine, and industry (Rinaudo, 2006; Muzzarelli, 2011). In terms of extraction, enzymatic techniques provide a more ecological and efficient way to isolate chitosan. Enzymatic hydrolysis, for example, breaks down the proteins present in the shells, facilitating the extraction of chitosan through filtration and purification (Synowiecki & Al-Khatteb, 2003). Another common method is the use of chitinase enzymes to directly degrade chitin, optimised by controlling conditions such as temperature and pH (Wang & Xu, 2006). Beyond its extraction, chitosan is notably distinguished by

its antioxidant capabilities, neutralizing free radicals and minimizing oxidative stress damage (Yen et al., 2008). These properties enhance the body's natural defense and open up potential applications in the food and cosmetic industries for their anti-aging and moisturizing benefits. Industrially, chitosan is employed for its antibacterial properties in food preservation (Jeon et al., 2002), improving the resistance and durability of textiles (Sandford, 1989), and in the fabrication of medical devices due to its hemostatic properties (Ko et al., 2000). In cosmetics, its effects on skin elasticity and aging make it a valuable addition to creams and lotions (Muzzarelli et al., 1999). In summary, chitosan is a versatile material with multiple potential applications across various sectors due to its unique and beneficial properties (Berger et al., 2004). The objectives of the present study were to prepare chitosan from shrimp scraps using an enzymatic route with pepsin, a porcine enzyme. The main goal was to characterize the prepared chitosan, assess its antioxidant activity, degree of deacetylation, molecular weight, viscosity, and crystalline structure by XRD, and finally study its structure and morphology using scanning electron microscopy.

## 2. MATERIALS AND METHODS

Chemicals phosphoric acid  $H_3PO_4$ , pork pepsin (SIGMA -ALDRICH - P7125), and all further chemicals and reagents were obtained from Sigma Chemical Co. Preparation of chitin and chitosan Shrimp shells were collected from local fisheries and fish markets in the Tlemcen region (Algeria). The shrimp shells are manually separated from the meat and then rinsed in cold water to eliminate impurities. Subsequently, they are dried at 10 to 20°C with adequate ventilation and a relative humidity of 50%. The dried shrimp shell samples are grounded using a waring 800ES mixer, resulting in a powder with a diameter ranging from 0.5 to 1 mm (Synowiecki & Al-Khatteb, 2003). After that, the shells are kept for further use at -18°C in stomacher vacuum bags (Wang & Xu, 2006).

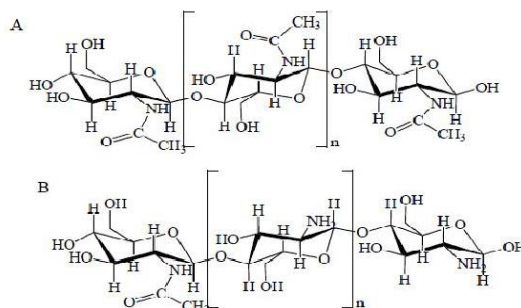


**Figure 1. The structure of completely acetylated chitin (A) and chitosan (B)**

### 2.1. Enzymatic extraction by acid proteolysis

This step aims to carry out the demineralization and deproteinization in a single phase in an acid medium. Demineralization is carried out using phosphoric acid  $H_3PO_4$  (Synowiecki & Al-Khatteb, 2003). Ten grams of the raw material sample was mixed with 60.32 mL of phosphoric acid at 0.9 mol/L. The mixture was heated to 50°C, and the process parameters were stabilized at around 50°C and pH 2 for 10 minutes. The enzyme was then added to the reaction medium under magnetic stirring in an oven for 6 hours. The enzyme concentration was 3% (relative to the weight of raw material), the temperature was set at 50°C, and the size of the exoskeleton fragments was less than 1 mm. The mixture was then filtered and rinsed abundantly with distilled water (Wang & Xu, 2006).

## 2.2. Deacetylation

Deacetylation is the procedure by which acetyl groups are removed from chitin. The obtained samples are deacetylated using a modified version of the established method (Salman, Ulaiwi, & Qais, 2018) after enzymatic deproteinization. The isolated chitin sample is treated with solutions of sodium hydroxide (NaOH) (SIGMA-ALDRICH) in concentrations spanning from 50% to 1:10 (p/v). The treated samples are subsequently autoclaved at 15 KPa and 121°C for 30 minutes. Subsequently, the samples are desiccated in a container overnight at 50°C, washed to a pH of 7, and weighed in an oven. Determination of chitosan deacetylation DD% Fourier transformed infrared (FTIR) spectroscopy (Bruker Alpha-T) was used to analyse the chitosan samples in the 400–4000 per cm range (Kumar et al., 2004). To create a salt disc with a diameter of 10 mm, 10 g of chitosan samples were combined with 100 g of dried potassium bromide (KBr) and compressed. Before spectrum reading, the discs were dried in a desiccator and heated to 80°C in an oven for sixteen hours. The DD was determined using the absorbances at 1655 and 3450  $\text{cm}^{-1}$  and the following equation (Brugnerotto et al., 2001):

$$\text{DD}\% = 100 - \left[ 100 \times \left( \frac{A_{1655}}{A_{3450}} \right) / 1.33 \right] \quad (01)$$

The absolute heights of the amide and hydroxyl absorption bands are  $A_{1655}$  and  $A_{3450}$   $\text{cm}^{-1}$ , respectively, and the degree of deacetylation is expressed as DD%.  $A_{1655}/A_{3450}$  for fully acetylated chitosan is 1.33.

## 2.3. Chitosan intrinsic viscosity and molecular weight (Mw)

An osculated tube viscometer was used to measure the viscosity of the chitosan solution at a temperature of 25°C (Paduretu et al., 2019). The molecular weights (MW) were calculated using the above equation, and the results are expressed in centipoises (cPs).

$$\text{Mv} = \frac{\eta}{k} * \frac{1}{a} \quad (02)$$

$\eta$ : viscosity of the sample,  $1.81 \times 10^{-5}$   $\text{cm}^3/\text{g}$  and 0.93 the values of K and a respectively.

## 2.4. X-ray diffraction measurement

The chitosan sample was verified, and the crystallinity index was assessed using XRD. Analysis was conducted using an X-ray diffractometer (Rigaku X-ray diffraction apparatus) with 40 kV of generating voltage and 40 mA of tube current. The device was powered by Cu  $K\alpha$  radiation at  $\lambda = 1.5406 \text{ \AA}$ , and samples were measured in the conventional continuous mode at  $2\theta$  angles between 05 and 45° (Thirugnanasambandan & Alagar, 2011). The duration of each step was 0.5 s, and the size of each step was 0.007°. The crystallinity index (ICr) was calculated using the following equation (Kasaai, 2008):

$$\text{ICr} = \frac{I_{110} - I_{am}}{I_{110}} * 100 \quad (03)$$

$I_{110}$  indicates the highest intensity at  $2\theta=20^\circ$ , while  $I_{am}$  refers to the amorphous diffraction intensity at  $2\theta=16^\circ$ .

## 2.5. Scanning electron microscopy (SEM)

For in-depth surface morphology investigations, the JEOL JCM-5000 scanning electron microscope, which operates at 5 kV and 20 kV, provides high-resolution imaging with magnification ranges of 18x to 60,000x. To achieve the best imaging results, sample preparation involves drying, mounting on SEM stubs, and

conductive coating (such as carbon or gold). The process entails setting up the microscope, calibrating it, and taking SEM pictures at different magnifications to emphasise the chitosan's macro and microstructural characteristics.

## 2.6. DPPH radical scavenging activity of chitosan.

We use a range of concentrations of 0.25%, 0.50%, 0.75%, and 1% acetic acid (v/v) to dissolve the chitosan sample. We mix 1 mL of the produced solution with 0.2 mM of 2,2-diphenyl-1-picrylhydrazyl (DPPH) (Sigma-Aldrich Co., St. Louis, MO) (Brand-Williams, Cuvelier, & Berset, 1995). We vigorously mix the solutions for 15 seconds and then leave them to incubate at room temperature, protected from light, for 30 minutes. We then used a spectrophotometer (UV-1601PC, Shimadzu Corporation Co., Tokyo, Japan) (Molyneux, 2004) to detect the absorbance at 517 nm. The DPPH radical-scavenging ability was found by comparing the absorbance with and without samples and giving it a percentage. This was done at 4 °C. We adopted butylated hydroxytoluene (BHT) to compare the DPPH free radical-scavenging activity (Sanchez-Moreno, 2002). We use the following equation to calculate the percentage of inhibition of DPPH radical formation:

$$\% \text{ Inhibition} = (A_{\text{control}} - A_{\text{sample}}) / A_{\text{control}} \times 100 \dots \dots \dots (04)$$

Where:

By sample: Absorbance of the sample.

To control: Absorbance of negative control.

The 50% inhibitory concentration (IC<sub>50</sub>) is determined from the regression curve equation obtained by the inhibition percentages at different concentrations

## 3. RESULTS AND DISCUSSION

### 3.1. Moisture, Protein, Ash Content, and Molecular Weight of Chitosan

The effectiveness of the enzymatic extraction conditions for chitosan from shrimp shell waste is determined by biochemical quality analysis. The moisture, protein, ash content, and molecular weight of the chitosan are presented in Table 01. The yield of chitosan was 17.16±0.21%, which is lower than that reported by Al-Hasan Hamdan et al., (2020), which was found to be 18-19%. This reduction could be attributed to the depolymerization of the chitosan polymer, loss of sample mass due to excessive removal of acetyl groups during deacetylation, and loss of chitosan particles during washing. The moisture content of the chitosan was 7.32±0.05%. This result indicates the chitosan's ability to absorb moisture from the atmosphere. Chitosan is hygroscopic in nature because the chemical groups in the chitosan structure can form hydrogen bonds with water (Salman et al., 2018). A better shelf life of chitosan is achieved by maintaining the moisture content below 10%. In this study, the ash content of the chitosan was 0.114±0.002%. The ash content limit for high-quality chitosan is less than 1% (Nouri et al. Furthermore, the ash content of the chitosan is directly correlated to the effectiveness of the demineralization process. The protein content of the chitosan was 1.12±0.02%. It indicates the effectiveness of the deproteinization in chitosan production. The average molecular weight of the chitosan estimated using intrinsic viscosity was 109.27±0.34KDa. Typically, the molecular weight of chitosan is higher than a million, while the range for commercial chitosan products varies from 100 KDa to 1,200 KDa (Renuka et al., 2019) . The solubility was 97.02±0.05% and is closely related to the degree of deacetylation and molecular mass, primarily because chitosan is actually a mixture of two polymers (chitin and chitosan) with different solubility behaviors. An increasing degree of deacetylation leads to higher chitosan content, which results in more amino groups and, consequently, increasing solubility in acetic acid solutions is expected (Pădurețu et al., 2019) (Baral et al., 2023)

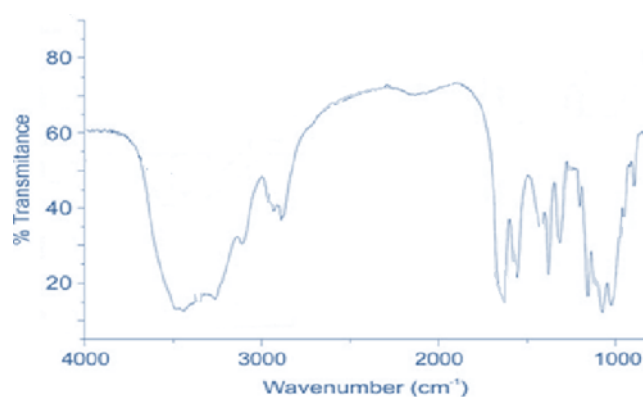
**Table 1: Physicochemical properties of chitosan**

Yield%	Moisture %	Ashes %	Proteins%	M.W Kda	Solubility%	DD %
17.16±0.22	7.32±0.05	0.114±0.002	1.12±0.02	109.27±0.34	97.02±0.05	87.13±0.16

### 3.2. FTIR spectral analysis

The structural confirmation of prepared chitosan is crucial for understanding its properties and potential applications. Fourier-transform infrared spectroscopy (FTIR) analysis is a powerful tool used to characterize the chemical structure of chitosan. In the FTIR spectra of chitosan (figure 2), distinctive absorption bands provide valuable insights into its molecular composition and functional groups (Kumar et al., 2004). Chitosan's absorption spectrum usually has clear peaks at certain wavenumbers, which show that the polymer has many chemical bonds and functional groups. For instance, the broad absorption band around 3423.24 cm<sup>-1</sup> corresponds to the stretching vibrations of OH groups in water and hydroxyls and the stretching vibrations of NH groups from free amines (Rinaudo, 2006). Another significant peak observed at 2922.26 cm<sup>-1</sup> is attributed to the asymmetric stretching of CH<sub>3</sub> and CH<sub>2</sub> groups within the prepared chitosan, indicating specific structural characteristics (Duarte et al., 2002).

Additionally, the intense peak at approximately 1656.34 cm<sup>-1</sup> signifies the NH<sub>2</sub> bending vibration, a distinctive feature of chitosan polysaccharides, and suggests the occurrence of deacetylation in the polymer structure (Brugnerotto et al., 2001). Further analysis reveals peaks at 1425.29 cm<sup>-1</sup> corresponding to C-H stretching and 1382.30 cm<sup>-1</sup> representing amide III due to C-N stretching in N-acetyl-glucosamine (Paulino et al., 2006). The absorption peak at 1151.29 cm<sup>-1</sup> indicates a symmetric glycosidic linkage (C-O-C), while an absorption band at 1027.12 cm<sup>-1</sup> signifies stretching vibrations of the C-O ring (Wan, 2008). Moreover, the absorption peak around 896.13 cm<sup>-1</sup> is associated with the glycosidic linkage of the β-(1-4) anomeric configuration (C-O-C), providing further insights into the chitosan structure and composition (Kasaai, 2008). This detailed FTIR analysis, as supported by various studies, enhances our understanding of the molecular characteristics of chitosan and its potential applications in diverse fields.

**Fig 2.** FTIR spectrum of chitosan

### 3.3. Analysis of Chitosan's Crystalline Structure using X-ray Diffraction

The XRD diffraction pattern of natural chitosan typically exhibits two distinct peaks at  $2\theta = 10^\circ$  and  $20^\circ$  (figure 3), indicating an organized crystalline structure (Mogilevskaya et al, 2006). This finding is supported by the research of Kasaai, (2008) who stated that the presence and intensity of these peaks at  $10^\circ$  and  $20^\circ$  are indicative of the degree of crystallinity in the chitosan sample. In addition, another study by Wang et al (2022) reported that chitosan can be readily modified through various physical or chemical methods, which may affect the degree of crystallinity. Furthermore, the study by Rasweefali et al (2021) also highlights the use of infrared spectroscopy to determine the degree of N-acetylation for chitosan. The FT-IR results mentioned in one of the sources indicate the presence of acid groups in treated samples. The XRD diffraction pattern of natural chitosan is consistent with previous findings, which indicate an organized crystalline structure characterized by distinct peaks at  $2\theta = 10^\circ$  and  $20^\circ$ . It is worth noting that the sources provided do not directly compare the XRD diffraction patterns of natural chitosan. However, they do provide valuable information on the degree of crystallinity in chitosan samples and the various techniques used to determine it.

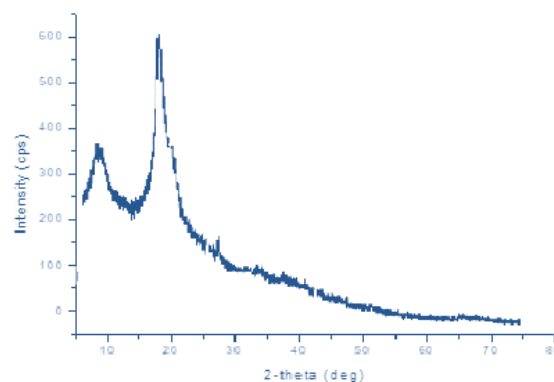


**Figure 3:** XRD diffraction of nanoparticle's chitosan

### 3.4. Scanning electron microscopy (SEM)

Scanning electron microscopy is a powerful technique that has been widely used for the characterization and analysis of various materials, including chitosan (Arzate-Vázquez, 2012). When applied to chitosan samples, scanning electron microscopy allows for the examination of the surface morphology and structural features at a high magnification (Sharma et Bhardwaj, 2019). The results of scanning electron microscopy analysis of chitosan (figure 4) revealed a distinctive surface morphology with a rough texture. The chitosan particles appeared to have irregular shapes and varying sizes, ranging from small granules to larger flakes. In addition, the scanning electron microscopy images showed that the chitosan particles had a porous structure, which could provide increased surface area and potential for adsorption. The presence of pores in chitosan particles allows for enhanced interactions with other substances, making it a suitable material for various applications such as adsorbents in water treatment, drug delivery systems, and tissue engineering scaffolds. These findings highlight the potential of chitosan as a versatile material with unique structural characteristics.



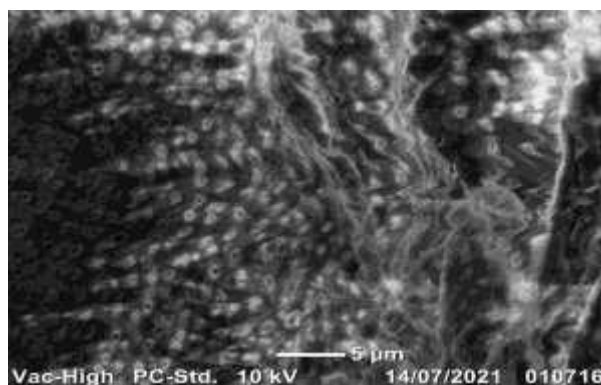


**Fig 4:** Scanning electron microscopy of chitosan

### 3.5. DPPH radical scavenging activity of chitosan

Antioxidant activity was assessed using the DPPH (2,2-diphenyl-1-picrylhydrazyl) test, a commonly employed method in laboratories to evaluate the antioxidant capacity of compounds (Brand-Williams, Cuvelier, & Berset, 1995). Antioxidants can neutralize free radicals like DPPH, indicating their scavenging potential. The reference antioxidant used was BHA (butylhydroxyanisole), a well-known antioxidant, serving as a benchmark to compare the antioxidant activity of chitosan against BHA (Yen et al., 2008). Chitosan's scavenging ability on DPPH radicals was measured at 72% at a concentration of 1%, indicating high antioxidant activity with significant neutralization of DPPH radicals (Huang et al., 2005). BHA exhibited scavenging abilities ranging from 45% to 85%, suggesting moderate to high, yet variable, antioxidant activity. Chitosan's antioxidant activity ranged from 39% at the lowest concentration (0.25%) to 72% at the highest concentration (1%), demonstrating an increase in activity with concentration. Park et al. (2004) suggest that chitosan can effectively eliminate or reduce free radicals or oxidative agents, supporting the findings in figure 5. In summary, these results suggest that chitosan is a promising natural antioxidant. Its effectiveness increases with concentration and can reach comparable or even superior levels to BHA, a commonly used synthetic antioxidant. This underscores its potential applications in areas requiring antioxidants, such as food preservation (Shahidi et al., 1999), cosmetics, or pharmaceutical applications to combat oxidative stress (Muzzarelli et al., 2007).

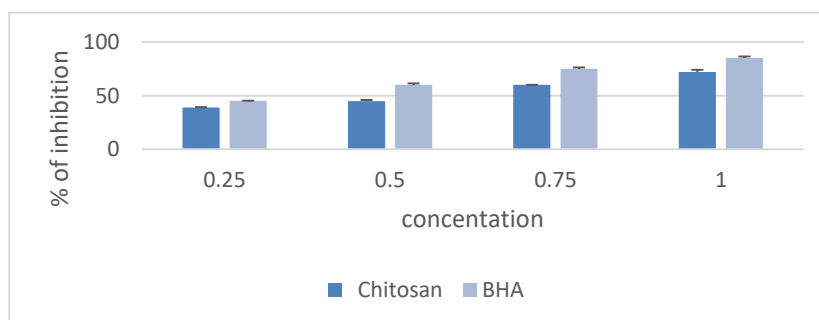


**Figure 5:** Scavenging activities of the chitosan from *Wastes*, BHA on DPPH radical.

Each test was replicated three times. The bar represented  $\pm$  SD.

#### 4. CONCLUSION

This study provides an in-depth analysis of chitosan extracted from shrimp shell waste through an enzymatic process. The yield of  $17.16 \pm 0.21\%$  aligns with the literature (18-19%). A moisture content of  $7.32 \pm 0.05\%$  demonstrates good absorption capacity while maintaining an adequate shelf life ( $<10\%$ ). The low ash ( $0.114 \pm 0.002\%$ ) and protein ( $1.12 \pm 0.02\%$ ) contents indicate effective deproteinization. The average molecular weight of  $109.27 \pm 0.34$  KDa falls within the commercial range (100-1200 KDa). The solubility of  $97.02 \pm 0.05\%$  in acetic acid is attributed to the high degree of deacetylation and molecular mass distribution. FTIR, XRD, and SEM analyses confirm the crystalline structure and porous morphology of the chitosan. Its high antioxidant activity (72% at 1%), comparable to BHA, opens prospects in the fields of food, pharmaceuticals, and biomaterials.

#### Acknowledgement

#### Author contributions

Dr. Fatma YUCEFI: conceived the presented idea, performed the experiments, analysed the data, and wrote the original draft of the paper. analysed the data, and critical revision of the article. KHERBACHE Atiqa: analysed the data of the article. All authors have read and approved the manuscript

#### Data availability

This published article contains all of the data generated or analyzed during this study.

#### Declarations

This work is supported by the Ministry of Higher Education and Scientific Research.

Conflict of interest: The authors declare that they have no conflict of interest.

#### 5. REFERENCES

1. Baral, A., Nayak, Y., Das, S. K., & Dash, S. (2023). Physicochemical and Biological Properties of Chitosan Extracted from Fish Scales of *Labeo Rohita*. *Journal of Survey in Fisheries Sciences*, 10(2S), 1769-1780.
2. Berger, J., Reist, M., Mayer, J. M., Fiechter, A., & Wintermantel, E. (2004). Chitosan: A versatile biopolymer for biomedical and pharmaceutical applications. *European Journal of Pharmaceutics and Biopharmaceutics*, 57(1), 35-52.
3. Brand-Williams, W., Cuvelier, M. E., & Berset, C. (1995). Use of a free radical method to evaluate antioxidant activity. *LWT - Food Science and Technology*, 28(1), 25-30.
4. Brugnerotto, J., Lizardi, J., Goycoolea, F. M., Arguelles-Monal, W., Desbrieres, J., & Rinaudo, M. (2001). An infrared investigation in relation with chitin and chitosan characterization. *Polymer*, 42(8), 3569-3580.



5. Duarte, M. L., Ferreira, M. C., Marvao, M. R., & Rocha, J. (2002). An optimised method to determine the degree of acetylation of chitin and chitosan by FTIR spectroscopy. *International Journal of Biological Macromolecules*, 31(1-3), 1-8.
6. Hamdan, I. A. A. H., Alhnon, F. J., & Hamdan, A. A. A. H. (2020, November). Extraction, characterization and bioactivity of chitosan from farms shrimps of Basra province by chemical method. In *Journal of Physics: Conference Series* (Vol. 1660, No. 1, p. 012023). IOP Publishing.
7. Huang, R., Mendis, E., & Kim, S. K. (2005). Factors affecting the free radical scavenging behavior of chitosan sulfate. *International Journal of Biological Macromolecules*, 36(1-2), 120-127.
8. Kasaai, M. R. (2008). A review of several reported procedures to determine the degree of N-acetylation for chitin and chitosan using infrared spectroscopy. *Carbohydrate Polymers*, 71(4), 497-508.
9. Kasaai, M. R. (2008). Various methods for determination of the degree of N-acetylation of chitin and chitosan: A review. *Journal of Agricultural and Food Chemistry*, 56(16), 7616-7629.
10. Ko, J. A., Park, H. J., Hwang, S. J., Park, J. B., & Lee, J. S. (2000). Preparation and characterization of chitosan microparticles intended for controlled drug delivery. *International Journal of Pharmaceutics*, 203(1-2), 195-204.
11. Kumar, M. R., Muzzarelli, R., Muzzarelli, C., Sashiwa, H., & Domb, A. J. (2004). Chitosan chemistry and pharmaceutical perspectives. *Chemical Reviews*, 104(12), 6017-6084.
12. Mogilevskaya, E. L., Akopova, T. A., Zelenetskii, A. N., & Ozerin, A. N. (2006). The crystal structure of chitin and chitosan. *Polymer Science Series A*, 48, 116-123.
13. Molyneux, P. (2004). The use of the stable free radical diphenylpicrylhydrazyl (DPPH) for estimating antioxidant activity. *Songklanakarin Journal of Science and Technology*, 26(2), 211-219.
14. Muzzarelli, R. A. A. (2011). Chitosan composites with inorganics, morphogenetic proteins and stem cells, for bone regeneration. *Carbohydrate Polymers*, 83(4), 1433-1445.
15. Nouri, M., Khodaiyan, F., Razavi, S. H., & Mousavi, M. A. (2016). The effect of different chemical and physical processing on the physicochemical and functional characterization of chitosan extracted from shrimp waste species of Indian white shrimp. *Progress in Rubber Plastics and Recycling Technology*, 32(1), 39-54.
16. Padurețu, C. C., Isopescu, R., Rău, I., Apetroaei, M. R., & Schröder, V. (2019). Influence of the parameters of chitin deacetylation process on the chitosan obtained from crab shell waste. *Korean Journal of Chemical Engineering*, 36, 1890-1899.
17. Padurețu, I., Popa, M. I., & Popa, N. (2019). Chitosan-based hydrogels for biomedical applications. *Journal of Materials Science: Materials in Medicine*, 30(4), 1-12.
18. Paulino, A. T., Simionato, J. I., Garcia, J. C., & Nozaki, J. (2006). Characterization of chitosan and chitin produced from silkworm chrysalides. *Carbohydrate Polymers*, 64(1), 98-103.

19. Rasweefali, M. K., Sabu, S., Sunooj, K., Sasidharan, A., & Xavier, K. M. (2021). Consequences of chemical deacetylation on physicochemical, structural and functional characteristics of chitosan extracted from deep-sea mud shrimp. *Carbohydrate Polymer Technologies and Applications*, 2, 100032.
20. Renuka, V., Ravishankar, C. N., Elavarasan, K., Zynudheen, A. A., & Joseph, T. C. (2019). Production and characterization of chitosan from shrimp shell waste of *Parapeneopsis stylifera*.
21. Salman, H. A., Venkatesh, S., Senthilkumar, R., Kumar, B. G., & Ali, A. M. (2018). Determination of antibacterial activity and metabolite profile of *Ruta graveolens* against *Streptococcus mutans* and *Streptococcus sobrinus*. *Journal of Laboratory Physicians*, 10(3), 320-325.
22. Sanchez-Moreno, C. (2002). Review: Methods used to evaluate the free radical scavenging activity in foods and biological systems. *Food Science and Technology International*, 8(3), 121-137.
23. Shahidi, F., Arachchi, J. K. V., & Jeon, Y. J. (1999). Food applications of chitin and chitosans. *Trends in Food Science & Technology*, 10(2), 37-51.
24. Sharma, V., & Bhardwaj, A. (2019). Scanning electron microscopy (SEM) in food quality evaluation. In *Evaluation technologies for food quality* (pp. 743-761). Woodhead Publishing.
25. Synowiecki, J., & Al-Khatteb, N. A. (2003). Production, properties, and some new applications of chitin and its derivatives. *Critical Reviews in Food Science and Nutrition*, 43(2), 145-171.
26. Thirugnanasambandan, T., & Alagar, M. (2011). Synthesis and characterization of chitosan-polyurethane semi-interpenetrating polymer network nanocomposites. *Journal of Applied Polymer Science*, 120(2), 1040-1048.
27. Wan, Y., Wu, H., Cao, X., & Dalai, S. (2008). Compressive mechanical properties and biodegradability of porous poly (caprolactone)/chitosan scaffolds. *Polymer Degradation and Stability*, 93(10), 1736-1741.
28. Wang, J., & Zhuang, S. (2022). Chitosan-based materials: Preparation, modification and application. *Journal of Cleaner Production*, 355, 131825.
29. Wang, S. L., & Xu, Y. (2006). Enzymatic production of chitosan from chitin. *Carbohydrate Polymers*, 64(1), 1-8.
30. Yen, M. T., Yang, J. H., & Mau, J. L. (2008). Antioxidant properties of chitosan from crab shells. *Carbohydrate Polymers*, 74(4), 840-844.